ISSN (Print) 1226-1750
ISSN (Online) 2233-6656
Journal of Magnetics 25(2), 126-132 (2020) https://doi.org/10.4283/JMAG.2020.25.2.126

Increase in Coercive Field by Magnetoelastic Coupling in Co/VO_2 Films

Won Jun Jung and Joonghoe Dho*

Department of Physics, Kyungpook National University, Daegu 41566, Republic of Korea

(Received 27 March 2020, Received in final form 29 May 2020, Accepted 1 June 2020)

Herein, a ferromagnetic cobalt (Co) film was deposited on a VO_2 film exhibiting a structural phase transition from monoclinic to tetragonal at ~340 K to investigate the magnetoelastic effect caused by a phase-transition-induced strain. First, (100) and (101) VO_2 films with thicknesses of 11-43 nm were grown on Al_2O_3 using pulsed laser deposition, and 2.5-nm-thick Co films were deposited on top of them via sputtering. The magneto-optic Kerr effect hysteresis loops were measured with the temperature variation across the structural phase transition temperature of VO_2. Upon heating, an increase in the coercive field of the Co layer was observed at the structural phase transition temperature of VO_2, suggesting a magnetoelastic coupling between the Co and VO_2 layers. The coercive field increment diminished with decreasing VO_2 thickness, and it disappeared as the VO_2 became thinner than a critical value of ~11 nm. These results imply that a phase-transition-induced strain in the VO_2 layer can be used to change the coercive field of the neighboring magnetic layer.

Keywords : magnetoelastic coupling, magnetic film, VO_2, structural phase transition

1. Introduction

Magnetic materials can display a change in their magnetic property via deformation (or lattice strain), i.e., the magnetoelastic effect (or inverse magnetostriction). A stress can be directly applied on a material to induce deformation, or it can be delivered to a neighboring material via elastic coupling between the two materials. In magnetic heterostructures, a strain-transfer behavior from a neighboring layer (or a substrate) to a ferromagnetic layer has been used to induce a magnetoelastic effect [1-3]. In particular, ferroelectric or piezoelectric materials were used to generate a controllable strain through an inverse piezoelectric effect [4, 5]. Although a strain of 0.1 - 0.5 % in piezoelectric materials is not large, the magnetoelastic effect was clearly observed in an epitaxially grown ferroelectric (or piezoelectric)/ferromagnetic bilayer. For example, a ferroelectric $BaTiO_3$ has a maximum strain of ~0.5 % when it undergoes a rhombohedral-to-orthorhombic transition at ~190 K and an orthorhombic-to-tetragonal transition at ~275 K. Previous works have demonstrated that such structural phase transitions induce a magnetization change in the neighboring magnetic films [6-8]. Similarly, piezoelectric materials, such as $PbZr_xTi_{1-x}O_3$ and $Pb(Mg_{1/3}Nb_{1/3})_{1-x}Ti_xO_3$, have been used to induce a magnetoelastic effect to the neighboring magnetic layer through an inverse piezoelectric effect controlled by an electric field [9-13].

Vanadium dioxide VO_2 exhibits a structural phase transition from monoclinic to tetragonal at a metal-insulator transition temperature T_{MI} of 340 K, which is accompanied by a change of ~0.7 % in the *c* lattice constant [14]. Polycrystalline or epitaxial VO_2 films can be grown on glass, silicon, sapphire, and TiO_2 substrates for various applications [15-19]. Interestingly, structural-transition-induced strain can modify the magnetization and the coercive field in ferromagnetic Ni or [Co/Pt] films coupled with VO_2 [20-23]. Recently, Venta reported that a Ni film coupled with VO_2 displayed a large coercive field change of 15 - 50 % at T_{MI} [21]. In addition, Wei reported that the perpendicular magnetic anisotropy in a [Co/Pt] film coupled with VO_2 disappeared as the temperature exceeded T_{MI} [23]. These results may be partly caused by the typical decreasing tendency of the magnetic strength of a magnetic material with increasing thermal fluctuation. Nevertheless, these reports suggest that the structural phase transition of VO_2 can generate a distinctive strain in the neighboring layer at the structural phase transition temperature, thus causing a magnetoelastic effect in the neighboring magnetic layer coupled with VO_2. Similarly,

*Corresponding author: Tel: +82-2-950-7354
Fax: +82-2-952-1739, e-mail: jhdho@knu.ac.kr

ferromagnetic Ni or Co films on V_2O_3 exhibited a change in their magnetization and coercivity because of phase-transition-induced strain [21]. The VO_2 thickness dependence of the magnetoelastic effect in ferromagnet/VO_2 systems has not been examined. In the current work, we investigated the temperature dependence of the coercive field of a Co layer coupled with 11-43-nm-thick VO_2 films. The increase in the coercive field of the Co layer at the structural phase transition temperature was attributed to a magnetoelastic effect in the Co layer, which was caused by a phase-transition-induced strain in VO_2. The increment disappeared when the VO_2 thickness decreased to a critical value of ~11 nm.

2. Experiments

Heteroepitaxial VO_2 films were prepared on Al_2O_3 substrates via pulsed laser deposition. Polycrystalline V_2O_3 and an Nd:YAG laser with a wavelength of 355 nm and a frequency of 1 Hz were used. During the deposition, the substrate temperature was fixed at 550 °C, and the oxygen partial pressure was maintained at 13 mTorr. Then, (100)- and (101)-oriented VO_2 films were grown on a C-plane Al_2O_3 and an R-plane Al_2O_3, respectively. [17, 18] Next, 2.5-nm-thick Co films were deposited on 43-, 22-, and 11-nm-thick VO_2 films using direct current (dc) sputtering at room temperature. The dc sputtering power was 20 W, and the Ar pressure was 4 mTorr. The root-mean-square roughness of the VO_2 films was about 1 nm. The temperature dependence of the resistance of the VO_2 films was investigated through four-point probe measurement in the temperature range of 290-380 K. The magnetic property of the Co layer coupled with VO_2 was investigated by a magneto-optic Kerr effect (MOKE) setup. The temperature dependence of the coercive field was obtained from the normalized MOKE hysteresis loop, which was measured upon heating and cooling.

3. Results and Discussions

Figure 1 shows the magnetic-field-dependent MOKE signals of the Co film on the 43-nm-thick (100) VO_2/C-plane Al_2O_3 at various temperatures from 300 to 380 K. The normalized MOKE signals were measured by applying a magnetic field along the easy-axis and hard-axis directions within the plane. For the easy-axis direction, the MOKE hysteresis loops at room temperature displayed a square-like shape with a saturation behavior of ~35 Oe. The saturation behavior along the hard-axis direction can be observed above ~75 Oe. As the temperature increased, the coercive field (H_C) values for both

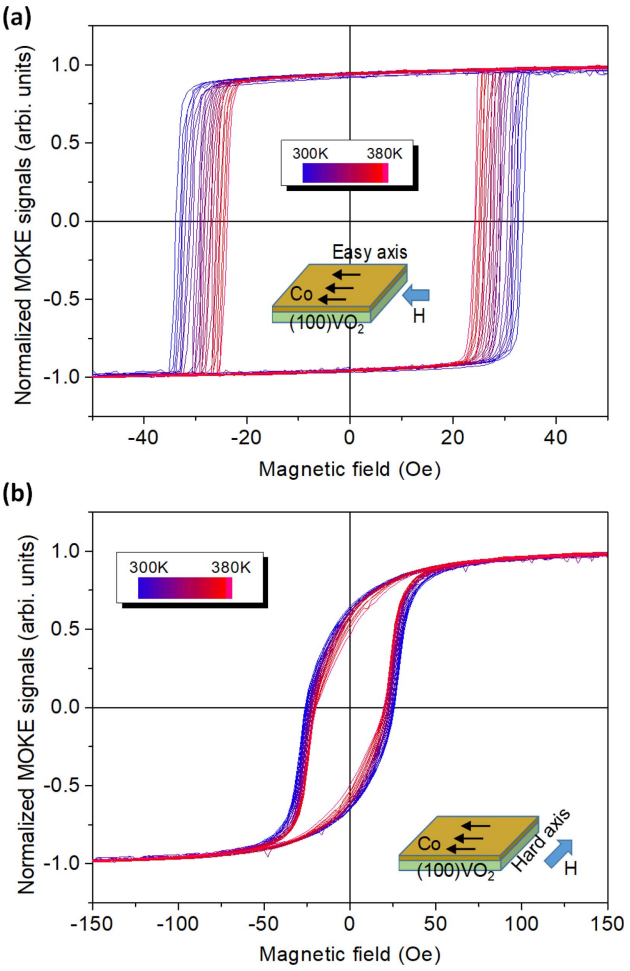

Fig. 1. (Color online) Magnetic field dependence of MOKE signals of Co film deposited on 43-nm-thick (100) VO_2/C-plane Al_2O_3 at various temperatures from 300 to 380 K (a) when the magnetic field (H) is parallel to an in-plane easy-axis direction and (b) when H is parallel to an in-plane hard-axis direction.

directions monotonously decreased. Figure 2 displays the temperature-dependent coercive field $H_C(T)$ of the Co film on the (100) VO_2/C-plane Al_2O_3 for the easy-axis and hard-axis directions. The H_C values were obtained with a repetitive temperature change of heating and cooling. The temperature-dependent resistance R(T) of the (100) VO_2 film on the C-plane Al_2O_3 substrate upon heating and cooling is also displayed. For the first heating, the $H_C(T)$ curve along the easy-axis direction exhibited a decreasing tendency with a slight slope change at T_{MI}. Presumably, the observed change in H_C at T_{MI} may be associated with a magnetoelastic coupling between Co and (100) VO_2, which was caused by the structural phase transition of VO_2 at T_{MI}. For the subsequent first cooling and second heating treatments, the $H_C(T)$ curve did not show a clear slope change at T_{MI}. The change at T_{MI}

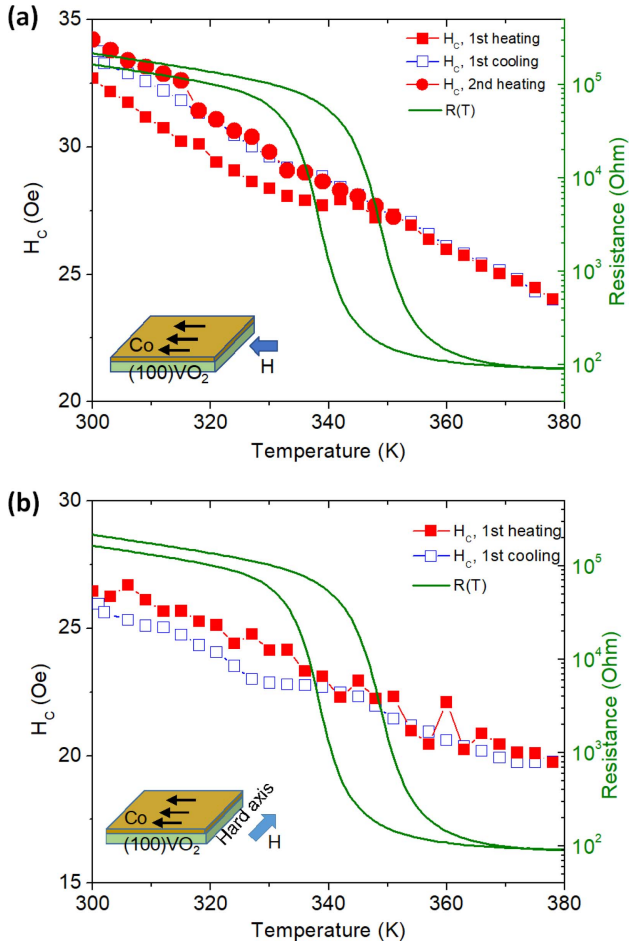

Fig. 2. (Color online) Temperature versus coercive field H_C of Co film deposited on 43-nm-thick (100) VO_2/C-plane Al_2O_3 (a) when the magnetic field H is parallel to an in-plane easy-axis direction and (b) when H is parallel to an in-plane hard-axis direction. The temperature dependence of the resistance R(T) of the (100) VO_2 on the C-plane Al_2O_3 is displayed together.

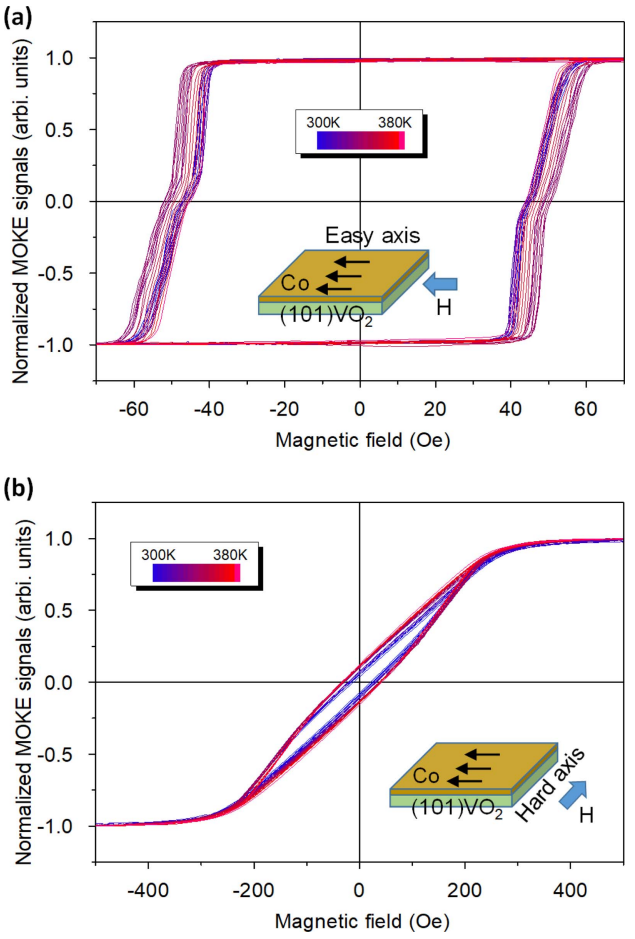

Fig. 3. (Color online) Magnetic field dependence of MOKE signals of Co film deposited on 43-nm-thick (101) VO_2/R-plane Al_2O_3 at various temperatures from 300 to 380 K (a) when the magnetic field (H) is parallel to an in-plane easy-axis direction and (b) when H is parallel to an in-plane hard-axis direction.

seemingly weakened by an irreversible change in the interface between the Co and (100) VO_2 after heating up to 380 K. For the hard-axis direction, the H_C(T) curve exhibited a decreasing tendency without any distinctive change at T_{MI}.

Figure 3 shows the magnetic-field-dependent MOKE signals of the Co film on the 43-nm-thick (101) VO_2/R-plane Al_2O_3 at various temperatures from 300 to 380 K. The normalized MOKE signals were measured by applying a magnetic field along the easy-axis and hard-axis directions within the plane. As the temperature increases, the MOKE hysteresis loops didn't now show a monotonous change but a rather anomalous change in the coercivity H_C. The (101)-oriented VO_2 films, with thicknesses of 43, 22, and 11 nm, were used to study the magnetoelastic coupling. Figure 4 displays the temperature-dependent coercivity, H_C(T), of the Co film on the (101) VO_2/R-plane Al_2O_3 substrate. As shown in the inset of Figure 4(c), the magnetic field was applied along the easy-axis direction. In all three samples, H_C(T) commonly exhibited a decreasing tendency with increasing temperature. For the first heating, remarkably, the H_C(T) of the Co film on the 43-nm-thick (101) VO_2 displayed a sudden increase from ~44 Oe to ~53 Oe at T_{MI}. Such a change at T_{MI} was reduced by the subsequent cooling and heating treatments. In addition, the change in the H_C value at T_{MI} was weakened in the sample with the 22-nm-thick (101) VO_2, and it was not observed in the sample with the 11-nm-thick (101) VO_2.

Figure 5 displays the temperature-dependent coercivity, H_C(T), of the Co film on the (101) VO_2/R-plane Al_2O_3 substrate in the hard-axis direction. The inset of Figure

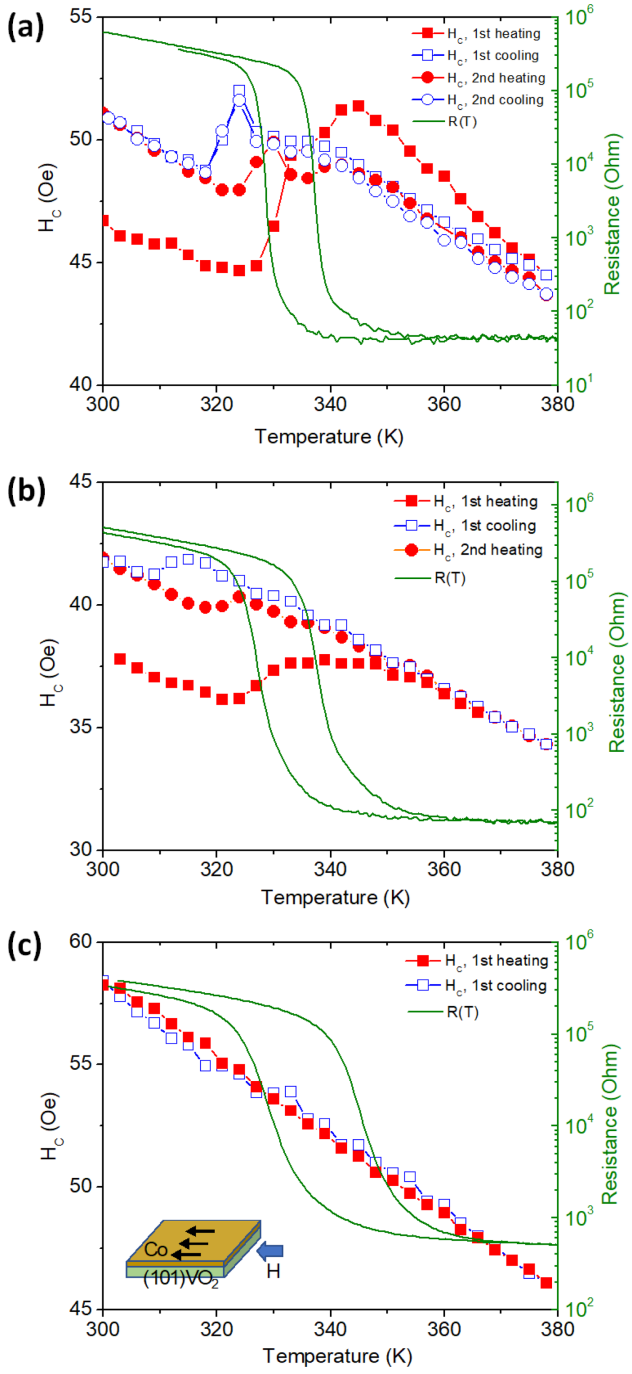

Fig. 4. (Color online) Temperature versus easy-axis coercive field H_C of Co film deposited on (a) 43-nm-, (b) 22-nm-, and (c) 11-nm-thick (101) VO_2/R-plane Al_2O_3. The temperature dependence of the resistance R(T) of the (101) VO_2 on the R-plane Al_2O_3 upon heating and cooling is displayed together.

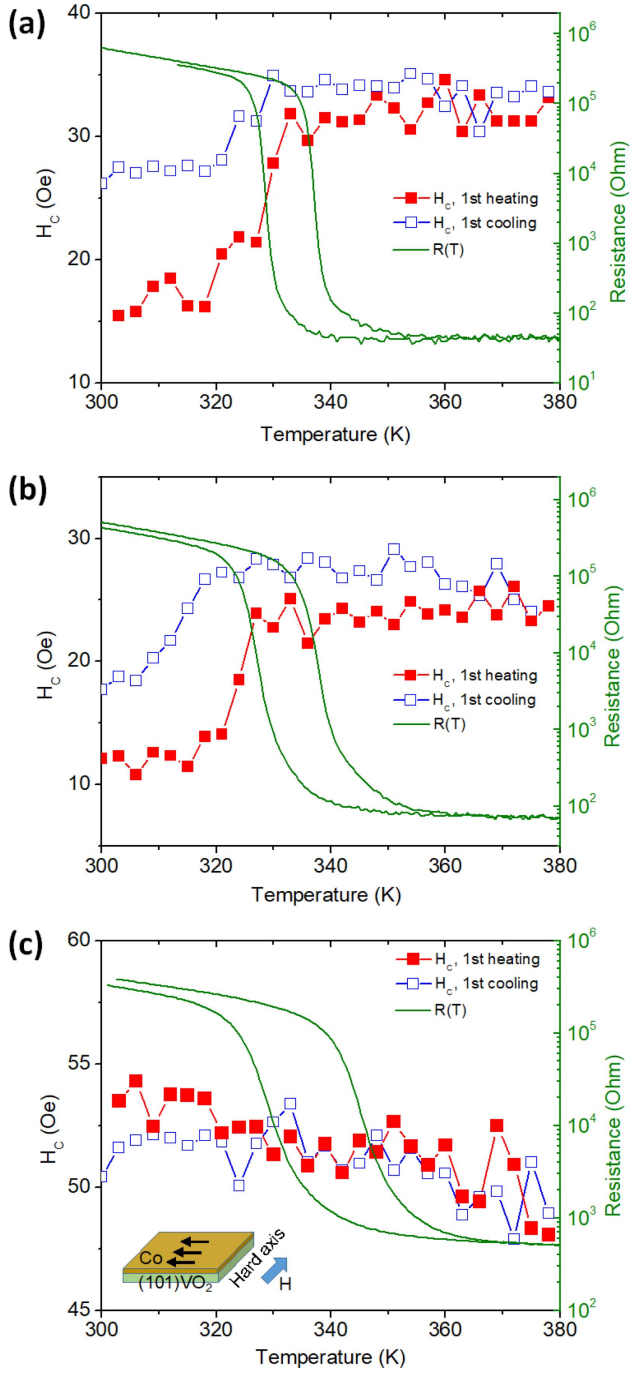

Fig. 5. (Color online) Temperature versus hard-axis coercive field H_C of Co film deposited on (a) 43-nm-, (b) 22-nm-, and (c) 11-nm-thick (101) VO_2/R-plane Al_2O_3. The temperature dependence of the resistance R(T) of the (101) VO_2 on the R-plane Al_2O_3 upon heating and cooling is displayed together.

5(c) shows a schematic picture of measurement configuration. For the first heating, the H_C(T) of the Co film on the 43-nm-thick (101) VO_2 displayed a sudden increase of about 10 Oe at T_{MI}. Similarly, the sample with the 22-nm-thick (101) VO_2 exhibited a small increment in the H_C value at T_{MI}, while the sample with the 11-nm-thick (101) VO_2 did not show an increase at T_{MI}. For the hard-axis direction, the change in the H_C value at T_{MI} also decreased in the cooling procedure after heating.

Figure 6 shows the relative change in the coercive field,

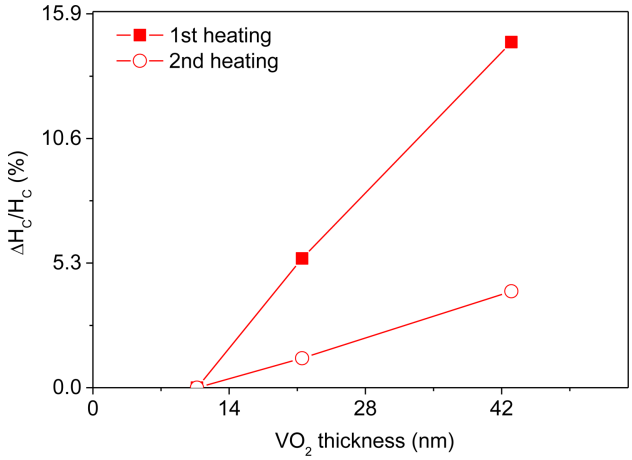

Fig. 6. (Color online) (101) VO_2 thickness versus relative change in coercive field, $\Delta H_C/H_C$, of Co layer along easy axis.

$\Delta H_C/H_C$, at T_{MI} with the VO_2 thickness. As the VO_2 thickness increased, the $\Delta H_C/H_C$ at T_{MI} displayed a linearly increasing tendency. A certain critical thickness was apparent around ~11 nm for the change in the coercive field at T_{MI}, implying that the magnetoelastic effect can only be observed if the VO_2 thickness is larger than this critical thickness. Previously, Yang *et al.* reported that a 60-nm-thick VO_2 film exhibited a sudden change in the lattice constant c with a structural phase transition from monoclinic to tetragonal, whereas a 13-nm-thick film did not show any indication of the structural phase transition at T_{MI} [19]. The absence of a structural phase transition in the thin VO_2 film was explained by an epitaxial stabilization of the tetragonal phase and an epitaxial strain. Therefore, we believe that the observed $\Delta H_C/H_C$ at T_{MI} with the VO_2 thickness is consistent with such previous results, and the temperature dependence of the coercive field in the Co layer is dependent on the structural phase transition property of the underlying VO_2 layer.

In the Co/VO_2 sample, the source of strain in the Co layer is the structural phase transition of the underlying VO_2 layer from a monoclinic to a rutile structure. As observed in Figs. 7(a) and (b), we estimated that the structural phase transition of the (100) VO_2 on the C-plane Al_2O_3 had approximate lattice parameter changes of +0.62 % and –0.7 % for the two in-plane orthogonal directions, whereas such transition of the (101) VO_2 on the R-plane Al_2O_3 had lattice parameter changes of +0.62 % and +0.19 %. Studies have shown that (100)-oriented rutile oxide films, such as TiO_2, VO_2, and CrO_2, could be heteroepitaxially grown on hexagonal C-plane Al_2O_3; however, they will have an in-plane texture because of the existence of three equivalent growth directions within the plane [24]. Therefore, we conjecture that the structural

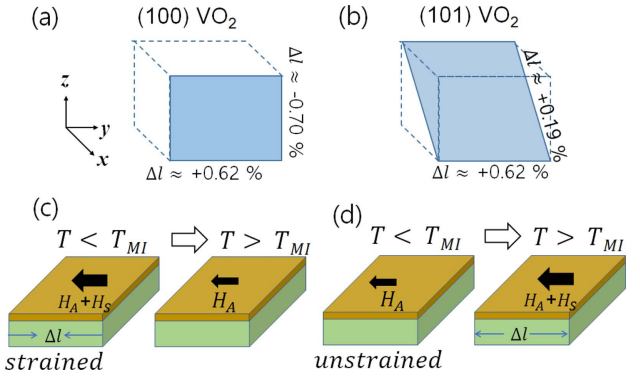

Fig. 7. (Color online) In-plane length change Δl of (a) (100) VO_2 on C-plane Al_2O_3 and (b) (101) VO_2 on R-plane Al_2O_3 caused by structural phase transition at T_{MI}. The in-plane length changes were estimated from the lattice parameters below and above T_{MI}. Schematic images for anisotropy field changes (c) from strained state to unstrained state and (d) from unstrained state to strained state. H_K and H_A represent a stress anisotropy field and a pre-existing anisotropy field, respectively.

phase transition of the underlying (100) VO_2 layer does not effectively generate lattice strain to the neighboring Co layer because two in-plane strains at the unit-cell scale are similar values with opposite signs. That is to say, we think that overall strain effect by small disordered (100) VO_2 grains within the plane is probably negligible because two opposite strain effect will be canceled out each other in a large scale. Presumably lots of small textured (100) VO_2 grains in the plane can't generate a homogeneous strain to the neighboring magnetic film as the single crystal-like (101) VO_2 film even in the plane. We hypothesize that the structural phase transition of the underlying (101) VO_2 on the R-plane Al_2O_3 can exert a strain effect on the neighboring Co layer through net in-plane strains at the unit-cell scale.

The lattice distortion in the underlying VO_2 layer generates an anisotropic stress on the neighboring Co layer. For the Co/(101)VO_2 on the R-plane Al_2O_3 sample in Fig. 4(a), the easy-axis coercivity increased from ~45 Oe at 325 K to ~52 Oe at 345 K. In addition, the hard-axis coercivity in Fig. 5(a) increased from ~20 Oe at 325 K to ~30 Oe at 345 K. We assume that the coercive field increment of +7 to +10 Oe between 325 and 345 K was due to the stress anisotropy field, which was caused by the structural phase transition of the VO_2 layer. A stress anisotropy effect can be added to other pre-existing anisotropy fields (H_A). The stress anisotropy field (H_K) is given by the expression [25]

$$H_K = \frac{3\lambda\sigma}{M_S}, \quad (1)$$

where σ is the stress in Pa, λ is the magnetostriction coefficient, and the saturation magnetization M_S is about 1400 emu/cm^3 (or 1400 × 10^3 A/m) for Co [26]. A net stress of −6.6 to −9.4 MPa would be required at 325 K to produce the +7 to +10 Oe (or 7 × 10^{-4} to 10^{-3} N/Am) anisotropy field for the Co/(101) VO_2 on the R-plane Al_2O_3 sample. This negative stress value is distinctively different from the positive stress of +22 MPa in the Ni/(100)VO_2 on the C-plane Al_2O_3 reported by Lauzier [20]. The magnetostriction coefficients for Co and Ni were reported to be about −50 × 10^{-6} and −34 × 10^{-6}, respectively [27]. Although both coefficients are negative, the effective stress can be an opposite type because of a difference in the pre-owned strain existing in the magnetic layer. In Lauzier's report, the Ni layer was deposited on VO_2 above T_{MI}; hence, it was in a contracted state below T_{MI} and in an unstrained state above T_{MI}, as shown in Fig. 7(c). In contrast, our Co film was deposited on VO_2 at room temperature; hence, it was in an unstrained state below T_{MI} and in an expanded state above T_{MI}, as shown in Fig. 7(d). A difference in the room temperature state may cause a variation in the pre-owned strain and the strain change with the temperature change across T_{MI}. Finally, we conjecture that the observed irreversible change of H_C upon heating and cooling treatments may be due to an imperfect adhesion with the deposition of the metallic Co on the oxide VO_2 at room temperature. An irreversible interfacial change can be induced when the measurement temperature becomes higher than the deposition temperature. Previously, Lauzier had reported that the irreversible change was very small when Ni films was deposited on VO_2 at 473 K [28].

4. Conclusions

In this study, 2.5-nm-thick Co films were deposited on (100) and (101) VO_2 films with thicknesses of 11-43 nm. The VO_2 films were used to induce magnetoelastic coupling with the Co layer because its structural phase transition from monoclinic to tetragonal has a phase-transition-induced strain of ~0.7 %. MOKE hysteresis loops were measured with a temperature change of up to 380 K. Upon heating, the coercive field of the Co layer displayed a sudden increase at ~T_{MI}, indicating a significant magnetoelastic coupling between the Co and VO_2 layers. However, this increment diminished with decreasing VO_2 thickness, and it disappeared as the VO_2 became thinner than a critical value of ~11 nm. Our results suggest that a phase-transition-induced strain in the VO_2 layer can be used to modify the coercive field in the neighboring magnetic layer.

Acknowledgments

This work was supported by The National Research Foundation of Korea (NRF-2018R1D1A1B07041955).

References

[1] H. Palneedi, D. Maurya, G.-Y. Kim, V. Annapureddy, M.-S. Noh, C.-Y. Kang, J.-W. Kim, J.-J. Choi, S.-Y. Choi, S.-Y. Chung, S.-J. L. Kang, S. Priya, and J. Ryu, Adv. Mater. **29**, 1605688 (2017).
[2] M. Liu, T. Nan, J.-M. Hu, S.-S. Zhao, Z. Zhou, C.-Y. Wang, Z.-D. Jiang, W. Ren, Z.-G. Ye, L.-Q. Chen, and N. X Sun, NPG Asia Mater. **8**, e316 (2016).
[3] K. Cai, M. Yang, and H. Ju, Nat. Mater. **16**, 712 (2017).
[4] C. Thiele, K. Dorr, O. Bilani, J. Rodel, and L. Schultz, Phys. Rev. B **75**, 054408 (2007).
[5] D. Bolten, U. Bottger, and R. Waser, J. Eur. Ceram. Soc. **24**, 725 (2004).
[6] W. Eerenstein, M. Wiora, J. L. Prieto, J. F. Scott, and N. D. Mathur, Nature Materials **6**, 348 (2007).
[7] H. F. Tian, T. L. Qu, L. B. Luo, J. J. Yang, S. M. Guo, H. Y. Zhang, Y. G. Zhao, and J. Q. Li, Appl. Phys. Lett. **92**, 063507 (2008).
[8] X. Moya, L. E. Hueso, F. Maccherozzi, A. I. Tovstolytkin, D. I. Podyalovskii, C. Ducati, L. C. Phillips, M. Ghidini, O. Hovorka, A. Berger, M. E. Vickers, E. Defay, S. S. Dhesi, and N. D. Mathur, Nature Mater. **12**, 52 (2013).
[9] H. J. A. Molegraaf, J. Hoffman, C. A. F. Vaz, S. Gariglio, D. van der Marel, C. H. Ahn, and J.-M. Triscone, Adv. Mater. **21**, 1 (2009).
[10] J. H. Park, Y. K. Jeong, S. Ryu, J. Y. Son, and H. M. Jang, Appl. Phys. Lett. **96**, 192504 (2010).
[11] J. L. Hockel, S. D. Pollard, K. P. Wetzlar, T. Wu, Y. Zhu, and G. P. Carman, Appl. Phys. Lett. **102**, 242901 (2013).
[12] W. Zhao, D. Zhang, D. Meng, W. Huang, L. Feng, C. Hou, Y. Lu, Y. Yin, and X. Li, Appl. Phys. Lett. **109**, 263502 (2016).
[13] S. P. Bennett, A. T. Wong, A. Glavic, A. Herklotz, C. Urban, I. Valmianski, M. D. Biegalski, H. M. Christen, T. Z. Ward, and V. Lauter, Sci. Rep. **6**, 22708 (2016).
[14] D. Kucharczyk and T. Niklewski, J. Appl. Crystallogr. **12**, 370 (1979).
[15] H.-T. Zhang, L. Guo, G. Stone, L. Zhang et al., Adv. Funct. Mater. **26**, 6612 (2016).
[16] A. Gupta, R. Aggarwal, P. Gupta, T. Dutta, Roger J. Narayan, and J. Narayan, Appl. Phys. Lett. **95**, 111915 (2009).
[17] Jian Li and J. Dho, Appl. Phys. Lett. **99**, 231909 (2011).
[18] Jian Li and J. Dho, J. Crystal Growth **404**, 84 (2014).
[19] M. M. Yang, Y. J. Yang, B. Hong, L. X. Wang, K. Hu, Y. Dong, H. Xu, H. Huang, J. Zhao, H. Chen, L. Song, H. Ju, J. Zhu, J. Bao, X. Li, Y. Gu, T. Yang, X. Gao, Z. Luo, and C. Gao, Sc. Rep. **6**, 23119 (2016).

[20] J. Lauzier, L. Sutton, and J. de la Venta, J. Appl. Phys. **122**, 173902 (2017).
[21] J. de la Venta, S. Wang, J. G. Ramirez, and I. K. Schuller, Appl. Phys. Lett. **102**, 122404 (2013).
[22] Y. J. Yang, B. Hong, H. L. Huang, Z. L. Luo, C. Gao, C. Kang, and X. Li, J. Mater. Sci. Mater. Electron. **29**, 2561 (2018).
[23] G. Wei, X. Lin, Z. Z. Si, N. Lei, Y. Chen, S. Eimer, and W. Zhao, Appl. Phys. Lett. **114**, 012407 (2019).
[24] J. Dho, J. Crys. Growth **311**, 2635 (2009).
[25] B. D. Cullity and C. D. Graham, Introduction to Magnetic Materials, 2nd ed. (John Wiley and Sons, Hoboken, New Jersey, 2008).
[26] M. Charilaou, C. Bordel, P.-E. Berche, B. B. Maranville, P. Fischer, and F. Hellman, Phys. Rev. B **93**, 224408 (2016).
[27] D. Sander, Rep. Prog. Phys. **62**, 809 (1999).
[28] J. Lauzier, L. Sutton, and J. de la Venta, J. Phys.: Condens. Matter **30**, 374004 (2018).